CYBERNETICS AND PHYSICS, VOL. 14, NO. 3, 2025, 299–307

STEAM PRESSURE CONTROL SYSTEM IN A COAL-FIRED THERMAL POWER PLANT WITH CROSS-LINKS

Denis Telichenko
Blagoveshchensk Cogeneration Station
Amur Generation Branch of Public Corporation DGK,
Russia
telichenko@yandex.ru

Sofya Zhigalova
Department of Information and Control Systems
Amur State University
Russia
sofya-books-1999@mail.ru

Evgeniy Shelenok
Higher School of Cybernetics and Digital Technologies
Pacific National University
Russia
cidshell@mail.ru

Larisa Nikiforova
Department of Information Security
Amur State University
Russia
chepak@inbox.ru

Article history:
Received 04.07.2025, Accepted 21.11.2025

Abstract

This article discusses the problem of designing a nonlinear combined controller for a steam pressure control system in the main pipeline of a thermal power plant. The mathematical model of this system is represented as a dynamic plant with a constant and known delay in control. The operation of this system takes place under conditions of structural and parametric uncertainties and switching. The hyperstability criterion and the approach for designing L-dissipative dynamic systems are used to develop dynamic feedback algorithms for a control scheme with an implicit reference model and correction filters. In the simulation stage, we conducted a simulation that clearly illustrated the quality of our control system.

Key words

thermal power plant, a priory uncertainty, switched system, input delayed plant, hyperstability criterion, correction filter

1 Introduction

Despite the rapid development of alternative energy sources, coal still accounts for a significant portion of global energy production. According to recent statistics, it accounts for approximately 34.4% of the world's total energy production [Graham et al., 2025]. A typical process of converting fossil fuels into electricity includes the use of a boiler, turbine, and generator. The main control task is to maintain steam pressure in front of the turbine, regardless of how much fuel is consumed, by adjusting the amount of fuel fed to the boiler [Basu and Debnath, 2019].

Load control options vary depending on factors such as the type of station, whether it is a block station or has a common steam main [Dukelow, 1991; Gilman, 2010]. In this paper, we discuss an approach for stations with a common collector, which is associated with the development of algorithms for the operation of a so-called main controller that acts on a heat load controller [Kolesnikova et al., 2019]. At the same time, it is assumed that each boiler has its own main regulator function, which can be either activated (boiler in control mode) or deactivated (boiler in standby mode). There are no cross-connections between the boilers.

The methodology of the present work is based on simulation and implementation of modern approaches for control of thermal power plants [Flynn, 2003; Wu et al., 2015]. The authors in the present article continue the research in the area of improving the algorithms for the main regulator of a coal-fired power plant with cross-connections (common collector and main steam line) [Eremin et al., 2022a; Eremin et al., 2022b]. Similar to [Eremin et al., 2022a], we consider the case when the control plant is multi-mode, including not only the technological section but also subordinate control loops [Kositsyn et al., 2013], whose operation mode is unknown and most accurately described by abruptly changing dynamics.

In this article, we focus on a broader class of plants, in contrast to previous research [Eremin et al., 2022a; Eremin et al., 2022b]. Thus, in [Eremin et al., 2022b],

the parameters of the plant were considered to be structurally and parametrically uncertain, without considering the switching mode. In [Eremin et al., 2022a], on the other hand, the multi-mode plant was considered, but it was limited by the constant relative degree. As will be shown below, in addition to expanding the functionality, we have proposed more universal and improved combined control laws. The technical implementation of these laws is simpler, and the quality of operation in tracking and stabilization modes is better.

2 Description of the technical area

Thermal power plants of the combined heat and power (CHP) class, which are designed to generate both heat and electricity, have a simple design and are characterized by the reliability and flexibility of their main equipment. These plants are typically coal-fired and have cross-connected systems. An example of such a power plant is the Blagoveshchenskaya TPP, the technological scheme of which is shown in Fig. 1

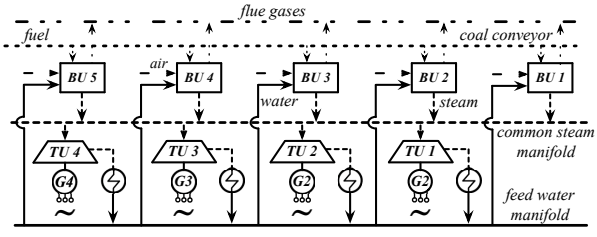

Figure 1. The structure of a typical cross-linked power plant.

The plant consists of boilers (*BU*) with a steam capacity of 420 t/h, turbine units (*TU*), together with generators (*G*) of various types with capacities ranging from 60 to 124 MW. The generators operate at a nominal pressure of 12.8 MPa, a superheated steam temperature of 555 ^{0}C, and a flow rate up to 520 t/h. The heat output of the plant exceeds 1,000 Gcal/h.

As mentioned above, for proper operation of the station, it is necessary to maintain steam pressure in the shared steam line, regardless of the configuration of turbine units and the dynamics of their operation. This is also necessary to account for deviations in the combustion and evaporation mode, as well as the presence of disturbances and cross-influences from all equipment operating on the shared steam line.

Let us examine in more detail the general structure of the main control systems in the technological process "air – dust (fuel) – water – steam", as shown in Fig. 2, which have a significant interdependence. Here: $*$ represents an optional signal; $f(...)$ represents a function that implements a specific control algorithm based on the input parameters; *CS* is the command signal; *MC* is the main controller; *Pm* is the pressure in manifold; *HLC/FC* is the heat load controller / fuel controller; *Ymc* is the output of the main controller that determines the boiler's load; *Pd* is the drum steam pressure; *Gcs* is the superheated steam consumption; *Ga* is the air consumption per boiler; *MLC* is the mill load controller; *Yhlc/fc* is the heat load controller output, which is an adjusted setting of the boiler load; *Ihm-m** is the hammer mill max current; *RCF* is the revolutions of raw coal feeder; *PAC* is the primary air controller; *Ymlc* is the mill load controller output; *Ihm* is the hammer mill current; *Tdam* is the temperature of dust-air mixture; *Gpa* is the primary air flow; *GHBF* is the gate hot blast fan; *DAMTC* is the dust-air mixture temperature controller; *Ypac* is the primary air controller output; *CARD* is the cold air regulating damper; *GAR* is the general air controller; *VR* is the vacuum controller.

Note that the practical scheme for a full-scale automated control system is more complicated than that presented in [Eremin et al., 2022b], and is only partially reflected in Fig. 2.

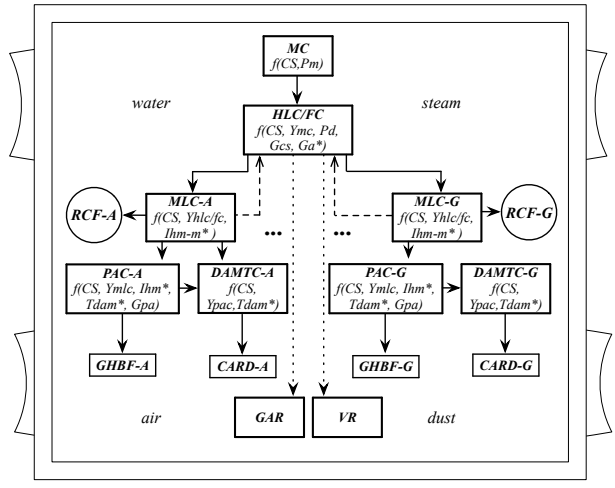

Figure 2. The structure of the combustion and evaporation process.

Regarding the process under discussion, several important points should be noted:

1. To decrease the system's response time, a proactive control mechanism can be implemented that simulates the expected response of the plant to an input signal. The controller then adjusts itself based on the error between the actual and expected responses.
2. The control loops are equipped with internal stabilizing controllers and corrective mechanisms, for example, to ensure accurate positioning of the actuator or compliance with other parameters and constraints.
3. The adjustment algorithms can be given by several sets of values, if necessary, to compensate for large deviations in the dynamics of the plant.

In general, control algorithms implemented in modern automated control systems involve setting a wide range of internal constraints to ensure shock-free operation of higher-level systems. These algorithms also take into account cross-links within the system and implement reference models and ensure the cascade operation of all automation systems. For example, for the circuit related to the heat load regulator *HLC/FC*, the fuel-to-air ratio is maintained. A top-down air flow signal *Ga**, can be used to control the airflow into the boiler.

Additionally, for this *HLC/FC* controller, load distribution functionality can be provided among all mills that are included in automatic operation. If, for some reason, the mill becomes unloaded (for example, because of the *Ihm-m** current limit provided in the circuit for each *MLC*), the task is then redistributed among the remaining machines that are still operating (due to the dotted communication lines). At the same time, it is possible to manually adjust the loading ratio for each mill and/or operate in tracking mode (where some of the control is automatic and some is manual).

For the primary air regulator *PAC* several cascade controllers can be set up in advance. These include those that ensure the amount of air supplied is proportional to the load (as estimated by the mill current), as well as those that provide temperature correction for the dust-air mixture. At the same time, it is still possible to ensure the operation of an independent cold air supply system for direct control of the dust-air mixture temperature.

We should note that the diagram in Fig. 2 is a simplified representation, but it is sufficient to illustrate the multi-mode operation of the system. Fuel regulators related to fuel oil (used for kindling and lighting in the event of a fire), temperature regulators for superheated steam behind the boiler, parts related to ventilation and purging, and other components are not included in this discussion. These can be considered as local systems.

Let us define the criteria by which a plant under consideration can be deemed structurally and parametrically uncertain, the mode of which changes abruptly, and which requires a separate study in order to develop high-quality control.

1. Studies conducted in practice have shown that, due to the operating mode of the object, it is difficult to define an unambiguous transfer function for it. In some cases, the 0/2 model was sufficient, while in others, 0/3 or 1/2 were more appropriate (the numbers refer to the order of the polynomials in the transfer function numerator and denominator). The basis for this conclusion was data from a passive experiment and information processing for a year's operation of one of the Blagoveshchenskaya TPP boilers.

2. Changing the order of the transfer function and its parameters is most often correlated not only with the load, but also with the operating modes of the subordinate control loops [Eremin et al., 2022a; Eremin et al., 2022b; Kositsyn et al., 2013; Nikolskiy and Telichenko, 2016]: for example, some of the mills were operating in automatic mode, while others were operating in manual mode (*MLC*, *PAC*, *DAMTC*, and *CARD* controllers). It should be noted that, in some cases, it is common practice to disable certain vacuum systems or operate them manually. This is done, among other reasons, to adjust the burning mode.

3. In addition to the analysis of experimental data, there is still the problem of improving the quality of fuel, for example, by adjusting its mixture, using non-standard types, which is relevant in today's conditions. As the experience of working in this mode has shown, the load changes by about 30%, and the dynamics of these changes can be abrupt.

4. It is also important to consider the fact that the control loop under consideration belongs to the highest control level, which is affected by both the operation of nearby systems (for example, the main air regulator (*GAR*) and dilution) as well as the operation of other boilers and turbines (see Fig. 1). This fact and its dynamics are difficult to predict and cannot be accurately described analytically.

Thus, from the perspective of creating a unified approach to pressure control in the common steam line with cross-connections, the most appropriate way to describe mathematically and dynamically is to consider a multi-mode, parametrically indefinite plant that allows for significant changes in its dynamics, in accordance with the practical experiment.

3 Initial and modified model of the plant

Let us represent the initial mathematical description of the parametric and structural indeterminate multi-mode plant as follows

$$\begin{gathered}\frac{d\mathbf{x}^{(k)}(t)}{dt} = \mathbf{A}^{(k)}\mathbf{x}^{(k)}(t) + \mathbf{B}^{(k)}u^{(k)}(t-\tau),\\ y^{(k)}(t) = \mathbf{C}_0^{(k)}\mathbf{x}^{(k)}(t),\ \ \mathbf{x}^{(k)}(0) = \mathbf{x}_0^{(k)},\end{gathered} \tag{1}$$

where $k = \overline{1,K}$ represent a limited number of time intervals $T_k = \left(t^k - t^{k-1}\right)$; $\mathbf{A}^{(k)}$, $\mathbf{B}^{(k)}$ and $\left(\mathbf{C}_0^{(k)}\right)^T$ represents state $\left(n^{(k)} \times n^{(k)}\right)$ matrices, control and output $n^{(k)}$ vectors like

$$\mathbf{A}^{(k)} = \begin{bmatrix} -a_1^{(k)} & 1 & 0 & ... & 0\\ -a_2^{(k)} & 0 & 1 & ... & 0\\ ... & ... & ... & ... & ...\\ -a_{n^{(k)}-1}^{(k)} & 0 & 0 & ... & 1\\ -a_{n^{(k)}}^{(k)} & 0 & 0 & ... & 0 \end{bmatrix},\ \mathbf{B}^{(k)} = \begin{bmatrix} b_0^{(k)}\\ b_1^{(k)}\\ ...\\ b_{m^{(k)}-1}^{(k)}\\ b_{m^{(k)}}^{(k)} \end{bmatrix},$$

$$\mathbf{C}_0^{(k)} = \begin{bmatrix}1 & 0 & ... & 0 & 0\end{bmatrix};$$

$\mathbf{x}^{(k)}(t) = \left[x_1^{(k)}(t)\ x_2^{(k)}(t)\ ...\ x_{n^{(k)}}^{(k)}(t)\right]^T$ represents a state vector; $u^{(k)}(t-\tau)$ and $y^{(k)}(t)$ represents scalar signals for control and output respectively; $\tau = const > 0$ represents input delay; $\mathbf{x}_0^{(k)}$ represents initial conditions.

We will assume that the plant (1) operates under following assumptions.

1. The matrix $\mathbf{A}^{(k)}$ and vector $\mathbf{B}^{(k)}$ are a priori unknown:

$$\mathbf{A}^{(k)} = \mathbf{A}^{(k)}(\xi),\ \mathbf{B}^{(k)} = \mathbf{B}^{(k)}(\xi),\ \xi \in \Xi, \quad (2)$$

where ξ are unknown parameters and Ξ is a known bounded numerical set.
2. τ is a known constant.
3. Only a delayed control signal and an output signal can be directly measured.
4. Transfer function of the control plant (*CP*) in the Laplace transform we can represent as

$$W_{CP}^{(k)}(s) = \frac{y^{(k)}(s)}{u^{(k)}(s)} = \frac{b_m^{(k)}(s)}{a_n^{(k)}(s)} \cdot e^{-s\tau}, \quad (3)$$

where s represents the Laplace transform variable; $b_m^{(k)}(s) = b_0^{(k)} s^{m^{(k)}} + b_1^{(k)} s^{m^{(k)}-1} + ... + b_{m^{(k)}}^{(k)}$ represents the Hurwitz polynomial with $b_0^{(k)} > 0$; $a_n^{(k)} = s^{(n^k)} + a_1^{(k)} s^{n^{(k)}-1} + ... + a_{n^{(k)}}^{(k)}$; $\deg b_m^{(k)}(s) = m^{(k)}$ and $\deg a_n^{(k)}(s) = n^{(k)}$ are unknown.
5. The relative degree of a transfer function (3) is a variable and belongs to a known range $1 \le \delta^{(k)} \le \overline{n} - \underline{m} = \overline{\delta}$; $\overline{n} = \max\left(\deg a_n^{(k)}\right)$, $\underline{m} = \min\left(\deg b_m^{(k)}\right)$ and therefore $\overline{\delta}$ are known.

In accordance with assumption 5, we will introduce an output correction filter (*OCF*) [Eremin, 2009; Eremin, 2013; **?**]. This dynamic unit has following form:

$$\tilde{y}^{(k)}(s) = W_{OCF}(s) y^{(k)}(s) = \left(\frac{Ts+1}{T_* s+1}\right)^{\overline{\delta}-1} y^{(k)}(s), \quad (4)$$

where $\tilde{y}^{(k)}(s)$ represents the filter output; $W_{OCF}(s)$ represent transfer function of the *OCF*; T and T_* are time constants, and T_* is small.

Considering the *OCF* model (4), the initial transfer function (3) can be transformed, by analogy with [Smirnova, 2021], as:

$$\overline{W}^{(k)}(s) = \frac{b_m^{(k)}(s)}{a_n^{(k)}(s)} \cdot e^{-s\tau} \cdot \left(\frac{Ts+1}{T_* s+1}\right)^{\overline{\delta}-1} = \frac{b_m^{(k)}(s) \cdot (Ts+1)^{\overline{\delta}-1}}{a_n^{(k)} \cdot (T_* s+1)^{\overline{\delta}-\delta^{(k)}}} \cdot e^{-s\tau} \times \times \frac{1}{(T_* s+1)^{\delta^{(k)}-1}} = W_{MCP}^{(k)}(s) \cdot W_{SDU}^{(k)}(s), \quad (5)$$

where $\overline{W}^{(k)}(s)$ represents the transfer function for serial connection *CP* (3) and *OCF* (4); $W_{MCP}^{(k)}(s)$ represents the transfer function for *modified control plant* (*MCP*) with relative degree equal to one: $\tilde{\delta} = n^{(k)} + \overline{\delta} - \delta^{(k)} - \left(m^{(k)} + \overline{\delta} - 1\right) = 1$; $W_{SDU}^{(k)}(s)$ represents a *structural disturbance unit* (*SDU*) for which in accordance with $T_* \ll 1$ [Eremin, 2009; Eremin, 2013; **?**] the identity $\frac{1}{(T_* s+1)^{\delta^{(k)}-1}}$ will be fair.

Thus, the modified model of the multi-mode plant under consideration in the extended state space we can represent as following:

$$\frac{d\tilde{\mathbf{x}}^{(k)}(t)}{dt} = \tilde{\mathbf{A}}^{(k)} \tilde{\mathbf{x}}^{(k)}(t) + \tilde{\mathbf{B}}^{(k)} u^{(k)}(t-\tau), \quad \tilde{y}^{(k)}(t) = \tilde{\mathbf{C}}_0^{(k)} \tilde{\mathbf{x}}^{(k)}(t),\ \ \tilde{\mathbf{x}}^{(k)}(0) = \tilde{\mathbf{x}}_0^{(k)}, \quad (6)$$

where $\tilde{\mathbf{A}}^{(k)}$, $\tilde{\mathbf{B}}^{(k)}$ and $\tilde{\mathbf{C}}_0^{(k)}$ has following structure:

$$\tilde{\mathbf{A}}^{(k)} = \begin{bmatrix} -\tilde{a}_1^{(k)} & 1 & 0 & ... & 0 \\ -\tilde{a}_2^{(k)} & 0 & 1 & ... & 0 \\ ... & ... & ... & ... & ... \\ -\tilde{a}_{m^{(k)}+\overline{\delta}-1}^{(k)} & 0 & 0 & ... & 1 \\ -\tilde{a}_{m^{(k)}+\overline{\delta}}^{(k)} & 0 & 0 & ... & 0 \end{bmatrix},$$

$$\tilde{\mathbf{B}}^{(k)} = \begin{bmatrix} \tilde{b}_0^{(k)} & ... & \tilde{b}_{m^{(k)}}^{(k)} & ... & \tilde{b}_{m^{(k)}+\overline{\delta}-1}^{(k)} \end{bmatrix}^T, \quad \tilde{\mathbf{C}}_0^{(k)} = \begin{bmatrix} 1 & 0 & ... & 0 & 0 \end{bmatrix};$$

$\tilde{\mathbf{x}}^{(k)}(t) = \left[\tilde{x}_1^{(k)}(t)\ \tilde{x}_2^{(k)}(t)\ ...\ \tilde{x}_{m^{(k)}+\overline{\delta}}^{(k)}(t)\right]^T$ and $\tilde{y}^{(t)}(t)$ are state vector and output of the *MCP*.

4 Reference Model and Predictor-Compensator

We will use a command signal $r(t)$ to generate the desired movement of the control plant. Dynamics of the main system's loop, due to the connection of the *OFC* (4), will be determined by the additional influence $\tilde{r}(t)$, which is the output of the following command correction filter (*CCF*) [Smirnova, 2021; Eremin, 2018]:

$$\tilde{r}(s) = W_{CCF}(s) r(s) = \left(\frac{Ts+1}{T_* s+1}\right)^{\overline{\delta}-1} r(s), \quad (7)$$

where W_{CCF} represents the *OCF* transfer function.

In this case we can use an implicit reference model [Fradkov, 1974]: $y_*^{(k)}(t) = \frac{\chi_*}{p+\chi_*}\tilde{r}(t)$, where $p = \frac{d}{dt}$; $y_*^{(k)}$ is the reference output; $\chi_* = const > 0$. Note, that if we set $\chi_* \gg 1$, then the identity $y_*^{(k)}(t) \cong \tilde{r}(t)$ will be fair. In the case under consideration we extend the state space of implicit reference using a polynomial

$\tilde{b}^{(k)}(p) = b_m^{(k)}(p)\,(Tp+1)^{\overline{\delta}-1}$ [Eremin, 2018; Eremin et al., 2010]:

$$\begin{gathered} y_*^{(k)}(t) = \frac{\chi_* \tilde{b}^{(k)}(p)}{(p+\chi_*)\,\tilde{b}^{(k)}(p)}\tilde{r}(t) \cong \\ \cong \frac{\hat{\chi}_* \tilde{b}^{(k)}(p)\tilde{b}^{(k)}_{m^{(k)}+\overline{\delta}-1}}{\tilde{a}^{(k)}(p)+\chi_*\tilde{b}^{(k)}(p)}\tilde{r}(t), \\ \hat{\chi}_* = \chi_* \left(\tilde{b}^{(k)}_{m^{(k)}+\overline{\delta}-1}\right)^{-1}, \\ \tilde{a}^{(k)}(p) = a_n^{(k)}(p)\,(T_*p+1)^{\overline{\delta}-\delta^{(k)}}. \end{gathered} \tag{8}$$

Then the reference (8) in the state-space form can be described as following:

$$\begin{gathered} \frac{d\mathbf{x}_*^{(k)}(t)}{dt} = \mathbf{A}_*^{(k)}\mathbf{x}_*^{(k)}(t) + \hat{\chi}_*\tilde{\mathbf{B}}^{(k)}\tilde{r}(t), \\ y_*^{(k)}(t) = \tilde{\mathbf{C}}_0^{(k)}\mathbf{x}_*^{(k)}(t),\ \mathbf{x}_*^{(k)}(0) = 0, \end{gathered} \tag{9}$$

where $\tilde{\mathbf{x}}_*^{(k)}(t) = \left[\tilde{x}_{*1}^{(k)}(t)\ \tilde{x}_{*2}^{(k)}(t)\ ...\ \tilde{x}_{*(m^{(k)}+\overline{\delta})}^{(k)}(t)\right]^T$ represents reference states; $\mathbf{A}_*^{(k)} = \tilde{\mathbf{A}}^{(k)} + \hat{\chi}_*\tilde{\mathbf{B}}^{(k)}\tilde{\mathbf{C}}_0^{(k)}$ represents Hurwitz matrix.

An important feature of the plant (1), (6) is the control channel delay. For compensation this delay we connect a *predictor-compensator* in parallel with control plant [Eremin et al., 2022b; Eremin, 2009; Eremin and Chepak, 2019]. The mathematical model of this unit is:

$$y_K^{(k)}(t) = \frac{\chi_*}{p+\chi_*}\left(u^{(k)}(t) - u^{(k)}(t-\tau)\right), \tag{10}$$

where $y_K^{(k)}(t)$ represents compensator's output signal. Following a similar to (8) transformations , we can represent the compensator model in the state-space like

$$\begin{gathered} \frac{d\mathbf{x}_K^{(k)}(t)}{dt} = \mathbf{A}_*^{(k)}\mathbf{x}_K^{(k)} + \\ + \hat{\chi}_*\tilde{\mathbf{B}}^{(k)}\left(u^{(k)} - u^{(k)}(t-\tau)\right), \\ y_K^{(k)}(t) = \tilde{\mathbf{C}}_0^{(k)}\mathbf{x}_K^{(k)}(t), \end{gathered} \tag{11}$$

where $\tilde{\mathbf{x}}_K^{(k)}(t) = \left[\tilde{x}_{K1}^{(k)}(t)\ \tilde{x}_{K2}^{(k)}(t)\ ...\ \tilde{x}_{K(m^{(k)}+\overline{\delta})}^{(k)}(t)\right]^T$.

5 Problem Statement

Let us formulate two control objectives for the system under consideration (1), (4), (6), (7), (9), and (11).

The main control goal is to ensure high-precision tracking of the plant (1) output $y^{(k)}(t)$ for the command signal $r(t)$:

$$\left|r(t) - y^{(k)}(t)\right| \le \Delta_r,\ t \to \infty, \tag{12}$$

where $\Delta = const > 0$ represents the maximum allowable tracking error.

Auxiliary control goal is to synthesize an explicit form for control law $u(t) = u\left(\tilde{y}^{(k)}(t), u^{(k)}(t-\tau), \tilde{r}(t)\right)$ which allow to track the main system's loop output $\tilde{y}^{(k)}(t)$ for the signal $\tilde{r}(t)$:

$$\begin{gathered} \left|\tilde{r}(t) - \tilde{y}^{(k)}(t)\right| \cong \left|y_*^{(k)}(t) - \tilde{y}^{(k)}(t)\right| \le \Delta_{ML}, \\ t \to \infty,\ \Delta_{ML} = const > 0 \end{gathered} \tag{13}$$

6 Synthesis of Dynamic Feedback Algorithms

Let us use the hyperstability criterion [Popov, 1973] to synthesize the control algorithms for the system under consideration. According to the criteria methodology, we will perform three main stages.

First stage. Let us introduce a mathematical description of the state deviated system. To do this, we will introduce a misalignment signal $\mathbf{e}^{(k)}(t) = \left(\mathbf{x}_*^{(k)}(t) - \tilde{\mathbf{x}}^{(k)}(t) - \mathbf{x}_K^{(k)}\right)$ and perform subtraction for systems (9), (6) and (11). Then considering $\mathbf{A}_*^{(k)} = \tilde{\mathbf{A}}^{(k)} + \hat{\chi}_*\tilde{\mathbf{B}}^{(k)}\tilde{\mathbf{C}}_0^{(k)}$, the mathematical description of the system can be written as following:

$$\begin{gathered} \frac{d\mathbf{e}^{(k)}(t)}{dt} = \mathbf{A}_*^{(k)}\mathbf{e}^{(k)} + \tilde{\mathbf{B}}^{(k)}\mu^{(k)}(t),\ v^{(k)}(t) = \\ = \tilde{\mathbf{C}}_0^{(k)}\mathbf{e}^{(k)}(t) = \tilde{r}(t) - \tilde{y}^{(k)}(t) - y_K^{(k)}(t), \\ \mu^{(k)}(t) = \hat{\chi} + *\tilde{r}(t) + \chi_*\tilde{y}^{(k)}(t) - \hat{\chi}_* u^{(k)}(t) + \\ + (\hat{\chi}_* - 1)\,u^{(k)}(t-\tau), \end{gathered} \tag{14}$$

where $\mu^{(k)}(t)$ and $v^{(k)}(t)$ represents modified input and output signals respectively.

Second stage. Let us fulfill the positivity conditions for the system's (14) linear stationary part (*LSP*):

$$\mathrm{Re}\left(\tilde{\mathbf{C}}_0^{(k)}\left(j\omega\mathbf{E} - \mathbf{A}_*^{(k)}\right)\tilde{\mathbf{B}}^{(k)}\right) > 0,\ \forall\omega \ge 0, \tag{15}$$

where $j^2 = -1$; ω represents frequency; $\mathbf{E}$ represents an unit matrix of the appropriate size. The *LSP* frequency transfer function in accordance with $\chi_* \gg 1$ can be represented by the following approximated equation:

$$W_{LSP}^{(k)}(j\omega) \cong \frac{\chi_*}{j\omega + \chi_*}. \tag{16}$$

Then, the fulfillment of (15) for the first-order inertial link (16) is obvious: $\mathrm{Re}\left(W_{LSP}^{(k)}(j\omega)\right) = \frac{\chi_*^2}{\chi_*^2+\omega^2} > > 0,\ \forall\omega \ge 0$.

Third stage. Let us ensure the validity of V. M. Popov's integral inequality:

$$\begin{gathered} \eta^{(k)}(0,t) = -\int_0^t \mu^{(k)}(\varsigma)v^{(k)}(\varsigma)d\varsigma \ge \\ \ge -\left(\eta_0^{(k)}\right)^2 = const, \forall t > 0. \end{gathered} \tag{17}$$

The left side of (17), due to the setting of the control signal like $u^{(k)}(t) = \sum_{j=1}^{3} u_j^{(k)}(t)$, can be represented as following:

$$\begin{gathered}\eta^{(k)}(0,t) = \sum_{j=1}^{3} \eta_j^{(k)}(0,t) = \\ = \int_0^t \left(\hat{\chi}_* u_1^{(k)}(\varsigma) - \hat{\chi}_* \tilde{r}(\varsigma)\right) v^{(k)}(\varsigma) d\varsigma + \\ + \int_0^t \left(\hat{\chi}_* u_2^{(k)}(\varsigma) + \chi_* \tilde{y}^{(k)}(\varsigma)\right) v^{(k)}(\varsigma) d\varsigma + \\ + \int_0^t \left(\hat{\chi}_* u_3^{(k)}(\varsigma) - (\hat{\chi}_* - 1)\, u^{(k)}(\varsigma - \tau)\right) \times \\ \times\, v(\varsigma) d\varsigma.\end{gathered} \tag{18}$$

We define the first component $u_1^{(k)}(t)$ by following equation:

$$\begin{gathered}u_1^{(k)}(t) = h_{11} \tilde{r}(t) \int_0^t \tilde{r}(\varsigma) v^{(k)}(\varsigma) d\varsigma + \\ + h_{12} \tilde{r}^2(t) v^{(k)}(t), \;\; h_{11}, h_{12} = const > 0.\end{gathered} \tag{19}$$

Then for the first summand from (18) we can obtain following estimate:

$$\begin{gathered}\eta_1^{(k)}(0,t) = h_{11} \hat{\chi}_* \int_0^t \tilde{r}(\varsigma) v^{(k)}(\varsigma) \times \\ \times \int_0^{\varsigma} \tilde{r}(\theta) v^{(k)}(\theta) d\theta d\varsigma + \\ + h_{12} \hat{\chi}_* \int_0^t \tilde{r}^2(\varsigma) \left(v^{(k)}(\varsigma)\right)^2 d\varsigma - \\ - \chi_* \int_0^t \tilde{r}(\varsigma) v^{(k)}(\varsigma) d\varsigma \geq \\ \geq \frac{h_{11} \hat{\chi}_*}{2} \left(\int_0^2 \tilde{r}(\varsigma) v^{(k)}(\varsigma) d\varsigma\right)^2 - \\ - \hat{\chi}_* \int_0^t \tilde{r}(\varsigma) v^{(k)}(\varsigma)^{(k)} d(\varsigma) \pm \frac{\hat{\chi}_*^2}{2 h_{11} \hat{\chi}_*} \geq \\ \geq -\frac{\hat{\chi}_*^2}{2 h_{11} \hat{\chi}_*} = const, \; \forall t > 0.\end{gathered} \tag{20}$$

The second component $u_2^{(k)}(t)$ we synthesize as follows [Shelenok, 2024; Eremin et al., 2021]:

$$\begin{gathered}u_2^{(k)}(t) = h_{21} \tilde{y}^{(k)}(t) \int_0^t \tilde{y}^{(k)}(\varsigma) v^{(k)}(\varsigma) d\varsigma + \\ + h_{22} \left(\tilde{y}^{(k)}\right)^2 v^{(k)}, \; h_{21}, h_{22} = const > 0;\end{gathered} \tag{21}$$

and, by analogy with (20), estimate the second summand from (18) like

$$\begin{gathered}\eta_2^{(k)}(0,t) \geq \frac{h_{21} \hat{\chi}_*}{2} \left(\int_0^t \tilde{y}^{(k)}(\varsigma) v^{(k)}(\varsigma) d\varsigma\right)^2 + \\ + \chi_* \int_0^t \tilde{y}^{(k)}(\varsigma) v^{(k)}(\varsigma) d\varsigma \pm \frac{\chi_*^2}{2 h_{21} \hat{\chi}_*} \geq \\ \geq -\frac{\chi_*^2}{2 h_{21} \hat{\chi}_*} = const, \; \forall t > 0.\end{gathered} \tag{22}$$

The third component $u_3^{(k)}(t)$, which is formed in the following form:

$$\begin{gathered}u_3^{(k)}(t) = \\ = h_{31} u^{(k)}(t - \tau) \int_0^t u^{(k)}(\varsigma - \tau) v^{(k)}(\varsigma) d\varsigma + \\ + h_{32} \left(u^{(k)}(t - \tau)\right)^2 v^{(k)}(t), \\ h_{31}, h_{32} = const > 0;\end{gathered} \tag{23}$$

allows us to obtain a fair assessment

$$\begin{gathered}\eta_3^{(k)}(0,t) = \\ = \frac{h_{31} \hat{\chi}_*}{2} \left(\int_0^t u^{(k)}(\varsigma - \tau) v^{(k)}(\varsigma) d\varsigma\right)^2 + \\ + h_{32} \hat{\chi}_* \int_0^t \left(u^{(k)}(\varsigma - \tau) v^{(k)}(\varsigma)\right)^2 d\varsigma - \\ - (\hat{\chi}_* - 1) \int_0^t u^{(k)}(\varsigma - \tau) v^{(k)}(\varsigma) d\varsigma \geq \\ \geq \frac{h_{31} \hat{\chi}_*}{2} \left(\int_0^t u^{(k)}(\varsigma - \tau) v^{(k)}(\varsigma) d\varsigma\right)^2 + \\ - (\hat{\chi}_* - 1) \int_0^t u^{(k)}(\varsigma - \tau) v^{(k)}(\varsigma) d\varsigma \pm \\ \pm \frac{(\hat{\chi}_* - 1)^2}{2 h_{31} \hat{\chi}_*} \geq -\frac{(\hat{\chi}_* - 1)^2}{2 h_{31} \hat{\chi}_*} = const, \; \forall t > 0.\end{gathered} \tag{24}$$

Thus, according to estimates (20), (22) and (24), the integral inequality (17) will hold:

$$\begin{gathered}\eta^{(k)}(0,t) \geq -\frac{\hat{\chi}_*^2}{2 h_{11} \hat{\chi}_*} - \frac{\chi_*^2}{2 h_{21} \hat{\chi}_*} - \frac{(\hat{\chi}_* - 1)^2}{2 h_{31} \hat{\chi}_*} \geq \\ \geq -\left(\eta_0^{(k)}\right)^2 = const, \; \forall t > 0.\end{gathered}$$

Then, the synthesized control law we can write in the following combined form:

$$\begin{gathered}u^k(t) = h_{11} \tilde{r}(t) \int_0^t \tilde{r}(\varsigma) v^{(k)}(\varsigma) d\varsigma + \\ + h_{12} \tilde{r}^2(t) v^{(k)}(t) + \\ + h_{21} \tilde{y}_{sat}^{(k)}(t) \int_0^t \tilde{y}_{sat}^{(k)}(\varsigma) v^{(k)}(\varsigma) d\varsigma + \\ + h_{22} \left(\tilde{y}_{sat}^{(k)}(t)\right)^2 v^{(k)}(t) + \\ + h_{31} u^{(k)}(t - \tau) \int_0^t u^{(k)}(\varsigma - \tau) v^{(k)}(\varsigma) d\varsigma + \\ + h_{32} \left(u^{(k)}(t - \tau)\right)^2 v^{(k)}(t), \\ v^{(k)}(t) = \tilde{r}(t) - \tilde{y}_{sat}^{(k)}(t),\end{gathered} \tag{25}$$

where $\tilde{y}^{(k)}_{sat}(t)$ represents a modified with the help of saturation signal like:

$$\tilde{y}^{(k)}_{sat}(t) = sat\left(\tilde{y}^{(k)}(t)\right) = \begin{cases} y_0, & \tilde{y}^{(k)}(t) \geq y_0, \\ \tilde{y}^{(k)}(t), & \left|\tilde{y}^{(k)}(t)\right| < y_0, \\ -y_0, & \tilde{y}^{(k)}(t) \leq -y_0. \end{cases}$$

The rationale for this modification is based on the possibility of significant peak emissions from the *OCF* (4) output, which could disrupt the system [Khalil, 2002].

Since inequalities (15) and (17) hold, according to the hyperstability, the modified control system (6) – (9), (25) is hyperstable in a given class of uncertainty and for it both auxiliary (13) and main (12) are fair.

It should be noted that the choice of T_* (see (4) and (7)) [Eremin, 2009; Eremin, 2013; Eremin, 2022], will ensure the *L*-dissipativity of the initial control system (1) – (4), (7) – (9), (25) when a structural disturbance $W^{(k)}_{SDU}(s)$ takes place.

7 System Simulation

To carry out the simulation stage, we will provide a mathematical description of the *CP* (1) as a switched system of transfer functions obtained from a passive experiment [Eremin et al., 2022b; Nikolskiy and Telichenko, 2016]. Four switched transfer functions represent the plant model that are activated at following time intervals.

(1): $t_1 \in [0;\ 20000)$ s,

$$W^{(1)}_{CP}(s) = \frac{0.6626\,(776s+1)}{1528000s^3 + 190400s^2 + 738s + 1} \cdot e^{-28s};$$

(2): $t_2 \in [20000;\ 40000)$ s,

$$W^{(2)}_{CP}(s) = \frac{0.6626\,(428s+1)}{122500s^2 + 472s + 1} \cdot e^{-28s};$$

(3): $t_3 \in [40000;\ 60000)$ s,

$$W^{(3)}_{CP}(s) = \frac{0.6626}{13960s^2 + 222s + 1} \cdot e^{-28s};$$

(4): $t_4 \in [60000;\ 80000)$ s,

$$W^{(4)}_{CP}(s) = \frac{0.6626}{136700s^3 + 14910s^2 + 220s + 1} \cdot e^{-28s}.$$

Switching in the presented plant is accompanied by parametric and structural changes:

1. First and third switching: the relative degree of the transfer function ($\delta^{(1)} = 2 \to \delta^{(2)} = 1$; $\delta^{(3)} = = 2 \to \delta^{(4)} = 3$) and the order of its denominator ($n^{(1)} = 3 \to n^{(2)} = 2$; $n^{(3)} = 2 \to n^{(4)} = 3$) are change.
2. Second switching: the relative degree of the transfer function change ($\delta^{(2)} = 1 \to \delta^{(3)} = 2$) and the order of its denominator remain constant ($n^{(2)} = = n^{(3)} = 2$).

Based on this, the maximum value of the plant relative degree is $\overline{\delta} = 3$. Therefore, the model of *OCF* (4) and *CCF* (7) will be:

$$W_{CCF}(s) = W_{OCF}(s) = \left(\frac{Ts+1}{T_*s+1}\right)^2.$$

Let is perform simulation of the system using following command signal:

$$r(t) = 0.8\left(1 - e^{-0.0005t}\right) - \\ - 0.2\left(1 - e^{-0.0005(t-20000)}\right) + \\ + 0.4\left(1 - e^{-0.0005(t-40000)}\right).$$

As a result of the experiment series, we selected the predictor-compensator parameter like $\chi_* = 1000$ and the following parameters for the combined algorithm (25) and filter corrector:

$$h_{11} = 2000,\ h_{12} = 5500,\ h_{21} = 3000, \\ h_{22} = 3500,\ h_{31} = 200,\ h_{32} = 700, \\ T = 83,\ T_* = 30. \tag{26}$$

Time histories of the control system are shown in Fig. 3 – 5.

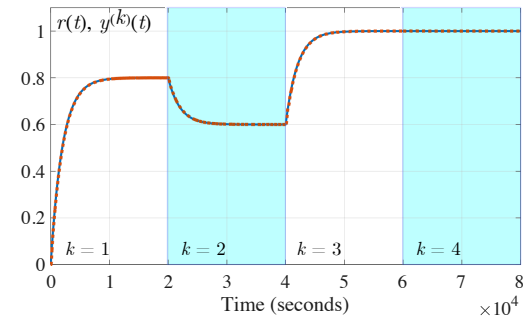

Figure 3. Command signal $r(t)$ (solid line), control plant output $y^{(k)}(t)$(dashed line).

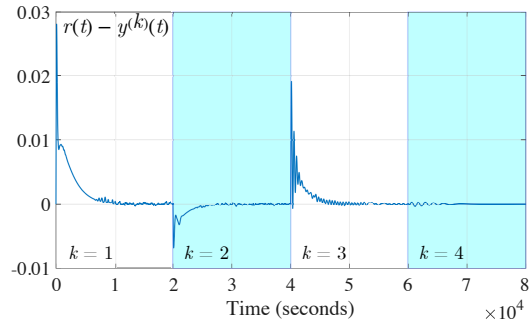

Figure 4. Mismatch between $r(t)$ and $y^{(k)}(t)$.

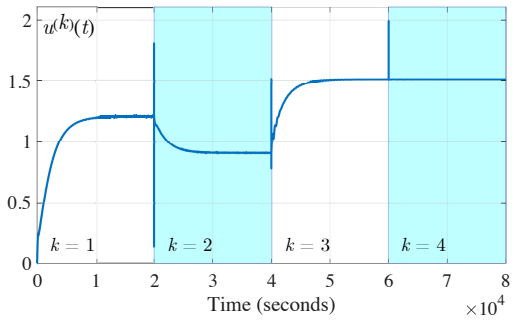

Figure 5. Control signal.

We should note that in order to test the most complex operating modes of the system, a theoretical task was set, as opposed to a practical one: tracking the task signal.

Simulation results demonstrate the high quality of the system's performance. In particular, Fig. 3 shows accurate tracking of the *CP* output for the command signal: the graphs of the two signals are almost identical. When the *CP* is switched, there are small spikes in the control error (see Fig. 4). However, in the steady state, the error does not exceed 0.05%.

8 Conclusion

It was designed and analyzed the structure and performance of a combined control algorithm for parametrically and structurally undefined multi-mode thermal power input-delayed plant. The advantage of the proposed control system is the ability to ensure a small steady-state error, as well as relative simplicity of implementation. This has been demonstrated at the simulation stage.

The solutions developed in this research will be effective in dealing with structural-parametric uncertainties in the event of delays and sudden changes in dynamics for thermal power plant and also high inertia plants.

Acknowledgements

This research was supported by the Ministry of science and higher education of the Russian Federation (project FEME-2024-0010).

References

Basu, S. and Debnath, A. K. (2019). *Power Plant Instrumentation and Control Handbook. A Guide to Thermal Power Plants. Second Edition*. Academic Press, Elsevier.

Dukelow, S. G. (1991). *The control of boilers. 2nd ed.* ISA – The Instrumentation, Systems, and Automation Society.

Eremin, E., Nikiforova, L., and Shelenok, E. (2021). Nonlinear repetitive control of the metal cutting machine feed module with saturated input. *Cybernetics and Physics*, **10** (4), pp. 240–247.

Eremin, E., Nikiforova, L., Telichenko, D., and Shelenok, E. (2022a). Adaptive control system for structurally undefined thermal power plant on set of functioning states. *Cybernetics and Physics*, **11** (2), pp. 67–73.

Eremin, E. L. (2009). *L*-dissipativity of adaptive systems with time delayed control and reference predictor (in Russian). *Informatika i Sistemy Upravlenia*, (2(20)), pp. 112–122.

Eremin, E. L. (2013). *L*-dissipativity of hyperstable control system in structural indignation. IV (in Russian). *Informatika i Sistemy Upravlenia*, (2(36)), pp. 100–106.

Eremin, E. L. (2018). Combined system with an imlplicit standard for a class of uncertain a priory single-channel non-affine control plants on the set of operations states (in Russian). *Informatika i Sistemy Upravlenia*, (3(57)), pp. 93–103.

Eremin, E. L. (2022). Method of large gain in the problem of self-organization of control systems of structurally indeterminate linear plants with switching. II (in Russian). *Informatika i Sistemy Upravlenia*, (2(72)), pp. 60–73.

Eremin, E. L. and Chepak, L. V. (2019). Combined controller for a nonaffine plant with delay in control. *Optoelectronics, Instrumentation and Data Processing*, **55** (6), pp. 542–549.

Eremin, E. L., Kvan, N. V., and Semichevskaya, N. P. (2010). Robust control of nonlinear object with high-speed obvious-implicit standart model (in Russian). *Mekhatronika, Avtomatizatsiya, Upravlenie*, (5), pp. 2–6.

Eremin, E. L., Nikiforova, L. V., Telichenko, D. A., and Shelenok, E. A. (2022b). A system for pressure controlling the common steam line of chp. In *2022 4th International Conference on Control Systems, Mathematical Modeling, Automation and Energy Efficiency (SUMMA)*, Lipetsk, Russia, pp. 826–831.

Flynn, D. (2003). *Thermal Power Plant Simulation and Control*. London, The Institution of Electrical Engineers.

Fradkov, A. L. (1974). Synthesis of adaptive system of stabilization for linear dynamic plants. *Automation and Remote Control*, **35**, pp. 1960–1966.

Gilman, G. F. (2010). *Boiler control systems. 2nd ed.* ISA – The Instrumentation, Systems, and Automation Society.

Graham, E., Fulghum, N., and Altieri, K. (2025). Global electricity review 2025.

Khalil, H. K. (2002). *Nonlinear Systems*. New Jersey, Prentice Hall.

Kolesnikova, O. V., Kazarinov, L. S., and Prosoedov, R. A. (2019). Automation of steam boiler load regulation at the electric power station of an iron and steel enterprise. In *2019 IEEE Russian Workshop on Power Engineering and Automation of Metallurgy Industry: Research & Practice (PEAMI)*, Magnitogorsk, Russia, pp. 110–115.

Kositsyn, V. Y., Rybalev, A. N., and Telichenko, D. A. (2013). A system for controlling the boiler heat load. *Thermal Engineering*, **60** (2), pp. 130–136.

Nikolskiy, D. I. and Telichenko, D. A. (2016). Mathematical models for one class of complex inertial objects with the changing dynamics and delay (in Russian). *Electronic scientific journal "Scientists notes PNU"*, **7** (3), pp. 142–151.

Popov, V. M. (1973). *Hyperstability of Control System*. Springer-Verlag, Berlin.

Shelenok, E. (2024). Combined repetitive control system for active damping of forced vibrations. *Cybernetics and Physics*, **13** (1), pp. 69–76.

Smirnova, S. A. (2021). Combined control system for the output of a linear plant with unknown relative order (in Russian). *Informatika i Sistemy Upravlenia*, (1(67)), pp. 114–125.

Wu, X., Shen, J., Li, Y., and Lee, K. Y. (2015). Steam power plant configuration, design, and control. *WIREs Energy Environ*, (4), pp. 537–563.